HHS Public Access

Author manuscript

Nature. Author manuscript; available in PMC 2010 January 09.

Published in final edited form as:

Nature. 2009 July 9; 460(7252): 225–230. doi:10.1038/nature08151.

CCR3 is a therapeutic and diagnostic target for neovascular age-related macular degeneration

Atsunobu Takeda[1,12], **Judit Z. Baffi**[1,12], **Mark E. Kleinman**[1,12], **Won Gil Cho**[1,12], **Miho Nozaki**[1,2], **Kiyoshi Yamada**[1], **Hiroki Kaneko**[1], **Romulo J.C. Albuquerque**[1,3], **Sami Dridi**[1], **Kuniharu Saito**[1], **Brian J. Raisler**[1,3], **Steven J. Budd**[4], **Pete Geisen**[4], **Ariel Munitz**[5], **Balamurali K. Ambati**[6,7], **Martha G. Green**[1], **Tatsuro Ishibashi**[8], **John D. Wright**[4], **Alison A. Humbles**[9,†], **Craig J. Gerard**[9], **Yuichiro Ogura**[2], **Yuzhen Pan**[10], **Justine R. Smith**[10], **Salvatore Grisanti**[11], **M. Elizabeth Hartnett**[4], **Marc E. Rothenberg**[5], and **Jayakrishna Ambati**[1,3]

[1]Department of Ophthalmology & Visual Sciences, Lexington, KY 40506, USA

[2]Department of Ophthalmology and Visual Science, Nagoya City University Graduate School of Medical Sciences, Nagoya 467-8601, Japan

[3]Department of Physiology, University of Kentucky, Lexington, KY 40506, USA

[4]Department of Ophthalmology, The University of North Carolina at Chapel Hill, Chapel Hill, NC 27599, USA

[5]Division of Allergy and Immunology, Department of Pediatrics, Cincinnati Children's Hospital Medical Center, University of Cincinnati, Cincinnati, OH 45229, USA

[6]Department of Ophthalmology and Visual Sciences, Moran Eye Center, University of Utah School of Medicine, Salt Lake City, UT 84132, USA

[7]Department of Ophthalmology, Veterans Affairs Salt Lake City Healthcare System, Salt Lake City, UT 84148, USA

[8]Department of Ophthalmology, Graduate School of Medical Sciences, Kyushu University, Fukuoka 812-8582, Japan

[9]Department of Medicine, Children's Hospital, Harvard Medical School, Boston, MA, 02215, USA

[10]Casey Eye Institute, Oregon Health and Science University, Portland, OR 97239, USA

[11]Department of Ophthalmology, University of Luebeck, D-23538 Lübeck, Germany

---

Author Information Correspondence and requests for materials should be addressed to J.A. (jamba2@email.uky.edu).

[12]These authors contributed equally to this work.

[†]Present address: Respiratory, Inflammation and Autoimmunity, Medimmune, Inc., Gaithersburg, MD 20878, USA.

Competing Interests Statement The authors declare competing financial interests.

Supplementary Information: Supplementary information accompanies this paper.

Author Contributions A.T., J.Z.B., M.E.K., W.G.C., M.N., K.Y., H.K., R.J.C.A., S.D., K.S., B.J.R., M.G.R., S.J.B., P.G., and A.M. performed experiments. S.G., A.A.H., Y.P., J.D.W., J.R.S, Y.O, T.I. provided reagents. J.A. conceived and directed the project, and, with assistance from B.K.A., M.E.H., M.E.R., R.J.C.A., and J.R.S. wrote the paper. All authors had the opportunity to discuss the results and comment on the manuscript.

Abstract

Age-related macular degeneration (AMD), a leading cause of blindness worldwide, is as prevalent as cancer in industrialized nations. Most blindness in AMD results from invasion of the retina by choroidal neovascularization (CNV). We report that the eosinophil/mast cell chemokine receptor CCR3 is specifically expressed in CNV endothelial cells in humans with AMD, and that, despite the expression of its ligands eotaxin-1, -2, and -3, neither eosinophils nor mast cells are present in human CNV. Genetic or pharmacological targeting of CCR3 or eotaxins inhibited injury-induced CNV in mice. CNV suppression by CCR3 blockade was due to direct inhibition of endothelial cell proliferation, and was uncoupled from inflammation as it occurred in mice lacking eosinophils or mast cells and was independent of macrophage and neutrophil recruitment. CCR3 blockade was more effective at reducing CNV than vascular endothelial growth factor-A (VEGF-A) neutralization, which is currently in clinical use, and, unlike VEGF-A blockade, not toxic to the mouse retina. *In vivo* imaging with CCR3-targeting quantum dots located spontaneous CNV invisible to standard fluorescein angiography in mice before retinal invasion. CCR3 targeting might reduce vision loss due to AMD through early detection and therapeutic angioinhibition.

AMD affects 30-50 million people globally, with approximately 90% of severe vision loss attributed to CNV1. The worldwide prevalence of CNV is expected to double in the next decade due to population aging. Targeting the pro-angiogenic cytokine vascular endothelial growth factor (VEGF)-A has been validated in patients with CNV2-4. However, substantial improvement of vision occurs only in one-third of patients treated with VEGF-A antagonists, and one-sixth of treated patients still progress to legal blindness. Moreover, safety concerns with continual blockade of VEGF-A, which is constitutively expressed in the normal adult human retina5, are emerging6,7. Thus, treatment strategies based on more specific targeting of CNV are desirable. However, no molecular marker specific for human CNV has yet been reported.

CCR3 expression restricted to CNV in human eyes

In our studies examining the role of chemokines in angiogenesis, we discovered that CCR3 (also known as CD193), a chemokine receptor best known for its role in promoting eosinophil and mast cell trafficking8, was expressed in human choroidal endothelial cells (CECs) only in the context of CNV due to AMD and not in other non-proliferating or proliferating choroidal vasculature (Fig. 1). Immunolocalization studies showed that CCR3 was expressed in CECs of all examined specimens of surgically excised CNV tissue from patients with AMD (18/18) who had received no prior treatment for AMD (Fig. 1a, b; Supplementary Fig. S1). In contrast, CCR3 was not expressed in CECs in the choroid of any patients with early (atrophic) AMD (0/10) or in age-matched patients without AMD (0/10) (Fig. 1c, d). CCR3 also was not immunolocalized in surgically excised tissue from patients with epiretinal fibrotic membranes (0/6) or in CECs in patients with choroidal melanoma (0/8) (Fig. 1e, f). Collectively these data point to a highly specific pattern of expression of CCR3 ($P = 7\times10^{-14}$, exact contingency table test) in CECs in neovascular AMD. In addition, we identified the expression of the CCR3 ligands eotaxin-1 (CCL11), -2 (CCL24), and -3 (CCL26) in all examined specimens of surgically excised CNV tissue from patients with AMD who had received no prior treatment for AMD (Fig. 1g-j), suggesting that the

eotaxin-CCR3 axis could play a role in this disease state. Interestingly, despite the abundance of eotaxins, eosinophils and mast cells were not identified in human CNV (Supplementary Fig. S2), consistent with earlier findings9.

CCR3 stimulation promotes CEC migration and proliferation

The best elucidated pathological functions of CCR3 to date have been its role in allergic diseases such as asthma10-14 and eosinophilic esophagitis15. There is a single report of its direct role in angiogenesis16. Although eosinophils and mast cells have been reported to be involved in angiogenesis17,18, such actions are considered minor or isolated. Therefore, we studied the effects of CCR3 modulation on angiogenesis *in vitro* and *in vivo*. Neutralizing anti-CCR3 antibodies inhibited the tube formation of primary human CECs cultured in Matrigel *in vitro* (Fig. 2a). In an experimental model of CNV induced by laser injury in wild-type mice19-24, neutralizing anti-CCR3 antibodies reduced the fraction of CECs *in vivo* that was in the proliferative state of the cell cycle (Fig. 2b). Consistent with this finding, each of the three eotaxins stimulated human CEC proliferation (Fig. 2c). Cytoskeletal rearrangement through polymerization of monomeric actin to microfilamentous F-actin, which is essential for eosinophil chemotaxis induced by the eotaxins, is also critical in angiogenic migration of endothelial cells. Stimulation of human CECs with any of the three eotaxins induced a rapid polymerization of actin molecules (Fig. 2d, e). All three eotaxins also activated Rac-1 (Supplementary Fig. S3), a small GTPase that is critical in regulating endothelial cell spreading and migration, and promoted human CEC migration in a dose-dependent fashion (Fig. 2f). Collectively these data demonstrate that CCR3 activation can promote multiple steps of angiogenesis. The expression of CCR3 on CECs *in vivo* is confined to CNV tissues; however, *in vitro*, human CECs responded to CCR3 ligands. This might be due to the presence of several CNV-promoting growth factors in the culture medium.

CCR3 receptor or ligand antagonism inhibits CNV

We studied the *in vivo* effects of CCR3 targeting in a mouse model of CNV induced by laser injury22 that is the most widely utilized animal model of this disease. A single intraocular administration of either CCR3 neutralizing antibodies or a small molecule CCR3 receptor antagonist ((S)-Methyl-2-naphthoylamino-3-(4-nitrophenyl)propionate) both suppressed laser injury-induced CNV in wild-type mice in a dose-dependent fashion (Fig. 3a-c). CNV was also diminished in $Ccr3^{-/-}$ mice25 compared to wild-type mice (Fig. 3d). The specificity of pharmacological CCR3 blockade was confirmed by demonstrating that CNV was not reduced in $Ccr3^{-/-}$ mice by CCR3 neutralizing antibodies or CCR3 receptor antagonist (116±7% and 109±16% of control, respectively; n = 5; $P > 0.1$). CCL-11 and CCL-24, the principal mouse ligands for CCR3, were markedly increased soon after laser injury and immunolocalized to the retinal pigmented epithelium (RPE), which is adjacent to CECs (Fig. 3e, f). Also, human RPE cells synthesized all three eotaxins (Supplementary Fig. S4), implicating these cells, which are abundantly interspersed in CNV9, as a source of CCR3 ligands in CNV. Genetic ablation of either *Ccl11* (ref. 26) or *Ccl24* (ref. 12) reduced CNV, while the neovascular response in $Ccl11^{-/-} \times Ccl24^{-/-}$ mice12 was suppressed to a greater extent than in either of the "single knockout" mice, suggesting cooperation between

these two ligands in this system (Fig. 3g). A single intraocular administration of neutralizing antibodies against CCL-11 or CCL-24 also suppressed CNV in wild-type mice (Fig. 3h, i), validating these CCR3 ligands as anti-angiogenic targets. Together, these data demonstrate that CCR3 activation is essential for *in vivo* angiogenesis in the most widely used preclinical model of neovascular AMD.

CCR3-driven angiogenesis uncoupled from inflammation

We sought to determine whether CCR3 targeting reduced CNV solely via anti-angiogenic mechanisms or whether anti-inflammatory mechanisms also were involved. Neither eosinophils nor mast cells (defined as $CCR3^{hi}CD3^{-}CD117^{int}CD49d^{+}$ and $CCR3^{int}CD3^{-}CD117^{hi}CD49d^{+}$ cells, respectively) were recruited to the choroid following laser injury, as monitored by flow cytometry (Supplementary Fig. S5). Furthermore, the CNV response in eosinophil-deficient Δ*dbl* GATA mice11 and mast cell-deficient $Kit^{W\text{-}v}/Kit^{W\text{-}v}$ mice27 was not different from that in wild-type mice (Fig. 3j). In addition, intraocular administration of neutralizing anti-CCR3 antibodies reduced CNV in Δdbl GATA or $Kit^{W\text{-}v}/Kit^{W\text{-}v}$ mice to the same extent as in wild-type mice. Thus, although eosinophils and mast cells have been reported to be capable of driving angiogenesis in other systems17,18, both cell types are dispensable in the development of experimental CNV. Although neutrophil and macrophage infiltration are crucial for the development of experimental CNV23,28, CCR3 receptor targeting did not affect recruitment of either inflammatory cell type (defined as $Gr\text{-}1^{+}F4/80^{-}$ and $F4/80^{+}CD11c^{-}$ cells, respectively) (Supplementary Fig. S5). Therefore, the angioinhibitory effect of CCR3 blockade in this model is a direct anti-vascular effect and does not appear to involve modulation of cellular inflammation. The mechanisms underlying the paucity of eosinophils and mast cells in CNV remain to be defined. One potential explanation could be the expression of CXCL9, which blocks eotaxin-induced CCR3-mediated eosinophil recruitment29,30, in CNV (Supplementary Fig. S6). Other mechanisms influencing adhesion or mobilization of these leukocytes also might be operative.

CNV bioimaging by CCR3 targeting

Because invasion of the retina by CNV results in morphological and functional disruption of the retina, early detection of CNV is desirable; indeed, detection of CNV before retinal invasion would be ideal. CNV that has breached the retina can be detected by fluorescein angiography. However, this diagnostic modality cannot detect CNV before it has invaded the retina, i.e., when it is still limited to the choroid. Yet postmortem histopathological studies have shown that substantial numbers of patients in whom fluorescein angiography does not reveal the presence of CNV nevertheless have CNV that has not yet invaded the retina31. Therefore, we explored whether CCR3-targeted bioimaging using anti-CCR3 Fab antibody fragments (Supplementary Fig. S7) conjugated to quantum dots (QDot-CCR3 Fab) could detect CNV before it became clinically evident.

We previously described the spontaneous development of CNV in senescent mice deficient in monocyte chemoattractant protein-1 (MCP-1/CCL-2) or its CCR2 receptor32. Similar pathology occurs at a younger age in $Ccl2^{-/-} \times Ccr2^{-/-}$ mice (unpublished data). These mice

also undergo outer retinal degeneration rapidly (Supplementary Fig. S8). We tested whether fundus angiography following intravenous injection of QDot-CCR3 Fab could detect subretinal CNV in these mice. QDot-CCR3 Fab angiography demonstrated hyperfluorescent signals in regions of the fundus of these mice that were silent on fluorescein angiography (Fig. 4a,b). The specificity of CCR3 targeting was confirmed by the absence of hyperfluorescent signals in *Ccl2*$^{-/-}$ × *Ccr2*$^{-/-}$ mice injected with QDot-isotype Fab and in wild-type mice injected with QDot-CCR3 Fab (Fig. 4b; Supplementary Fig. S9). Histological examination of these areas revealed proliferating (Ki67^{+}) CCR3^{+} blood vessels in the choroid that had not yet invaded the retina, along with accumulation of QDot-CCR3 Fab in these vessels (Fig. 4c-e). These data provide proof of principle that CCR3-targeted bioimaging can detect subclinical CNV before it disrupts the retina and causes vision loss.

CCR3 targeting superior to VEGF-A targeting

In comparing CCR3 targeting to VEGF-A targeting, the most effective approved treatment for human CNV, we found that CCR3 neutralizing antibodies were more effective than VEGF-A neutralizing antibodies (68±3% vs. 57±4%) at inhibiting laser-induced CNV in mice (Supplementary Fig. S10). In the laser injury model, CCR3 neutralization did not change VEGF-A levels in the RPE/choroid and VEGF-A blockade did not change CCR3 expression on CECs (Supplementary Fig. S11): these two pathways appear to be not directly coupled. Repeated intravitreous administration of anti-VEGF-A antibodies resulted in anatomic and functional damage to the retina in wild-type mice (Supplementary Fig. S12), consistent with earlier reports that anti-VEGF-A therapy induces dysfunction in and damage to the inner and outer murine retina6,7. These effects were modest at a dose of anti-VEGF-A antibodies that suppressed mouse CNV but more pronounced at a higher dose that is comparable to the dose used in humans. It should be noted that anti-VEGF-A pharmacotherapy has not been associated with an increased risk of profound retinal damage in humans33, but subtle abnormalities have been observed34,35 and some adverse effects might be misattributed to disease progression. In contrast to VEGF-A blockade, neither CCR3 Ab nor CCR3 receptor antagonist induced retinal toxicity in wild-type mice as confirmed by fundus imaging and electrophysiological function (Supplementary Fig. S12). *Vegfa* deletion is embryonically lethal36,37 and conditional ablation of *Vegfa* in the RPE induces profound retinal degeneration and visual dysfunction38. In contrast, the *Ccr3*$^{-/-}$ mouse retina was normal in appearance and electrophysiological function (Supplementary Fig. S13).

Discussion

Our findings suggest that CCR3 targeting may be a safe and viable strategy for early detection (using biocompatible quantum dots or other bioimaging fluorochromes such as near infrared dyes) and treatment of CNV (by receptor or ligand targeting) that might be superior to current standard of care. CCR3 bioimaging is likely to be most useful in individuals with RPE pigmentary disturbances and multiple subretinal lipoproteinaceous deposits known as drusen or fellow eye involvement with clinically evident CNV, as they are known to be at high risk for developing CNV39,40. Similar techniques might be useful

in non-invasively bioimaging other metabolic or molecular markers to provide information about disease pathogenesis or activity.

Several strategies have yielded molecular markers that are preferentially expressed on proliferating endothelial cells such as those in tumour vasculature41,42; however, CCR3 has not been identified in any of these reports. Therefore, our studies identify CCR3 as a novel marker of pathological angiogenesis and as a functional target in neovascular AMD. These findings also should prompt a search for genetic polymorphisms in the eotaxin-CCR3 axis in patients with AMD, and investigations of CCR3 function in other models of angiogenesis. Also, it is tempting to speculate that targeting CCR3 might provide dual benefits in asthma, which involves varying degrees of eosinophilic inflammation as well as angiogenic airway remodelling43.

Methods Summary

Mouse model of CNV

Laser photocoagulation (OcuLight GL, Iridex Corporation) was performed on mouse eyes to induce CNV, and CNV volumes were measured 7 days after injury by scanning laser confocal microscope (TCS SP, Leica) as previously described22.

Drug injections

Rat IgG2a neutralizing antibody against mouse CCR3 (R&D Systems), control rat IgG2a (Serotec), goat neutralizing antibody against mouse CCL11 (R&D Systems), goat neutralizing antibody against mouse CCL24 (R&D Systems), control goat IgG (Jackson Immunoresearch), or (S)-Methyl-2-naphthoylamino-3-(4-nitrophenyl)propionate (SB328437; Calbiochem) dissolved in DMSO were injected into the vitreous humor using a 33-gauge double-calibre needle (Ito Corporation) once, immediately after laser injury as previously described22.

CCR3 bioimaging

F(ab) fragments were created from monoclonal IgG2a antibody raised against the extracellular domain of murine CCR3 (R&D Systems) and an isotype rat IgG2a (R&D Systems) using a commercially available papain-based kit (Pierce). Recovered fragments were conjugated with quantum dots (Invitrogen, QDot-800) and resuspended in sterile PBS. *Ccl2*$^{-/-}$ × *Ccr2*$^{-/-}$ mice were administered 100 μg of tagged CCR3 F(ab) or isotype F(ab) via tail vein injection after acquiring baseline fluorescent imaging using a Topcon retinal camera (TRC-50IX). Serial images were then acquired at 1, 4, and 12 h after which eyes were harvested and frozen in OCT for immunofluorescent analyses. Retinal images were analyzed (ImageNet, Topcon) by comparison to baseline and fluorescein angiographic data. Hyperfluorescent areas were then cropped, equally thresholded, and pseudocoloured (Photoshop CS3, Adobe). Sections from QDot-conjugated CCR3 or rat IgG2a isotype F(ab) injected animals were fixed in 4% paraformaldehyde and blocked with 5% normal donkey serum/5% goat serum in PBS, stained with rat anti-mouse CD31 (BD Biosciences) and either rabbit anti-mouse CCR3 (Santa Cruz) or rabbit anti-Ki67 (Abcam) followed by

appropriate fluorescent secondary antibodies (Alexa Fluor 488/594, Invitrogen), and evaluated by confocal laser scanning microscopy (Leica SP-5).

Methods

Human tissue

Choroidal neovascularization (CNV) tissue was excised from patients with age-related macular degeneration (AMD) who had no prior treatment for CNV. Retinal fibrosis tissue was excised from patients with a diagnosis of epiretinal membrane formation. Donor eyes from patients with atrophic AMD without CNV and patients without AMD were obtained from eye banks. Eyes with choroidal melanoma were obtained by surgical enucleation. The study followed the guidelines of the Declaration of Helsinki. Institutional review boards granted approval for allocation and histological analysis of specimens.

Animals

All animal experiments were in accordance with the guidelines of the University of Kentucky IACUC and the Association for Research in Vision and Ophthalmology. C57BL/6J and $Kit^{W\text{-}v}/Kit^{W\text{-}v}$ mice were purchased from The Jackson Laboratory. $Ccr3^{-/-}$, $Ccl11^{-/-}$, $Ccl24^{-/-}$, $Ccl11^{-/-} \times Ccl24^{-/-}$, and Δdbl GATA mice have been previously described11,12,25,26. $Ccl2^{-/-} \times Ccr2^{-/-}$ mice were generated by interbreeding “single knockout” mice described previously32.

Drug injections

Rat IgG2a neutralizing antibody against mouse CCR3 (R&D Systems), control rat IgG2a (Serotec), goat neutralizing antibody against mouse CCL11 (1 μg; R&D Systems), goat neutralizing antibody against mouse CCL24 (5 μg; R&D Systems), control goat IgG (Jackson Immunoresearch), or (S)-Methyl-2-naphthoylamino-3-(4-nitrophenyl)propionate (SB328437; Calbiochem) dissolved in DMSO were injected into the vitreous humor of mice using a 33-gauge double-calibre needle (Ito Corporation) once, immediately after laser injury as previously described22.

Flow cytometry

Rat antibody against mouse CCR3 (1:250; Santa Cruz) coupled with PE-donkey antibody against rat IgG (1:250; Jackson Immunoresearch) or AlexaFluor647-conjugated rat antibody against mouse CCR3 (10 μg/ml; BD Biosciences) were used to quantify cell surface receptor expression on choroidal endothelial cells, defined by $CD31^+$ $VEGFR\text{-}2^+$ expression, gated by FITC-conjugated rat antibody against mouse CD31 (20 μg/ml; BD Biosciences) and PE-conjugated rat antibody against mouse VEGFR-2 (20 μg/ml; BD Biosciences). Macrophages, neutrophils, eosinophils and mast cells were defined as $F4/80^+CD11c^-$, $Gr\text{-}1^+F4/80^-$, $CCR3^{hi}CD3^-CD117^{int}CD49d^+$ and $CCR3^{int}CD3^-$ $CD117^{hi}CD49d^+$ cells, respectively. DNA content for cell cycle was analyzed after incubation with propidium iodide (0.05 mg/ml; Molecular Probes) containing 0.1% Triton X-100 and RNase A (0.1 mg/ml; Roche). Samples were analyzed on a LSRII (Becton Dickinson).

Immunolabeling

Immunofluorescent staining was performed with antibodies against human CCR3 (rat monoclonal, R&D Systems) or human CD31 (mouse monoclonal, Dako) and identified with Alexa 488 (Molecular Probes) or Cy3 secondary antibodies (Jackson ImmunoResearch). Immunohistochemical staining with the primary antibodies specific for human eotaxins-1, 2 and 3 (mouse monoclonal, R&D Systems) was performed using horseradish peroxidase. Laser injured mouse eye sections were stained with antibodies against mouse CCL11 or CCL24 (both R&D Systems) along with antibody against mouse CD31 (BD Biosciences) and visualized with FITC or Cy3 secondary antibodies. Images were obtained using Leica SP5 or Zeiss Axio Observer Z1 microscopes.

Tube formation assay

96-well plates were coated with Growth Factor Reduced Matrigel (BD Biosciences) mixed with rat neutralizing antibody against human CCR3 (20 μg/ml, R&D Systems) or control rat IgG2a (Invitrogen) and allowed to solidify in the incubator at 37 °C for 45 min. Human choroidal endothelial cells (CECs)44-47 were plated on top of the Matrigel at $2.25 \times 10^4/cm^2$ in EBM-2 basal media (Cambrex) containing 1% FBS with CCR3 antibody or rat IgG2a at the above concentrations and allowed to grow overnight. Tube formation was analyzed by counting the number of cell junctions per mm^2.

Proliferation assay

Human CECs were synchronized for cell cycle state by first cultivating them in EGM2-MV media (Lonza) supplemented with 10% FBS (Gibco) to achieve complete confluence and then by overnight serum starvation in MCDB131 media (Gibco) with 0.1% FBS. They were passaged to 96-well plates at a density of 5,000 cells per well, followed by stimulation for 24 h with eotaxin-1, 2 or 3 (10 ng, 100 ng and 2 μg per ml, respectively; Peprotech) in MCDB131 media with 0.1% FBS. After 24 h, cell viability was measured with BrdU ELISA (Chemicon) according to manufacturer's instructions.

F-actin Polymerization Assay

Human CECs were seeded in black-walled 96-well plates and grown to 70-80% confluence in fully supplemented EGM-2MV. Cultures were serum starved overnight in basal media and then stimulated with recombinant human eotaxin-1 (10 ng/ml), eotaxin-2 (100 ng/ml), eotaxin-3 (2 μg/ml) (Peprotech), or vehicle control (PBS). At 0, 10, 30, 60, or 120 sec time-points, cells were fixed in 3.7% paraformaldehyde for 10 min, washed, permeabilized in PBS with 0.1% Triton-X, and then stained with rhodamine labelled Phalloidin (1:200, Invitrogen) per manufacturer's recommendations. Plates were analyzed on a fluorescent plate reader (Synergy 4, Biotek) followed by fluorescent microscopy (Nikon E800).

Migration Assay

Eotaxins-1, -2, -3 were reconstituted in 0.1% bovine serum albumin (BSA) and then mixed with Matrigel diluted 1:1 with serum free endothelial basal media (EBM-2; Lanza). 500 μl of EBM-2 was added to each well of a 24-well plate followed by a 6.5 mm diameter Transwell insert (8 μm pores; Corning). Human CECs in EBM-2 were prestained with

Vybrant DiO (Invitrogen) for 30 min at 37 °C and seeded into the inserts at 50,000 cells per 200 μl of serum free EBM-2 media. The plates were allowed to incubate for 16 h at 37 °C, 5% CO_2. The migrated cells were imaged with an Olympus CK40 microscope and Olympus DP71 camera.

Rac-1 activation

Human CECs were cultured in EGM-2 MV containing 5% FBS. Prior to starting the assay, cells were serum starved with basal medium (MCDB131) supplemented with 1% FBS overnight. Cells were stimulated for designated times with Eotaxin-1, 2 and 3 (10 ng/ml, 100 ng/ml and 2 μg/ml respectively). Equal amounts of lysates (500 μg) were incubated with GST-Pak1-PBD agarose beads (Upstate) to pull-down active GTP-bound Rac-1 at 4 °C for 1 h with rotation. The samples were subsequently analyzed for bound Rac-1 by western blot analysis using an anti-Rac-1 antibody (Upstate).

Electroretinography

Mice were dark adapted overnight and then anesthetized. Both eyes were positioned within a ColorBurst Ganzfeld stimulator (Diagnosys). Espion software (Diagnosys) was used to program a fully automated flash intensity series from which retinal responses were recorded.

Supplementary Material

Refer to Web version on PubMed Central for supplementary material.

Acknowledgments

We thank R. King, L. Xu, M. McConnell, K. Emerson, G.R. Pattison, and M. Mingler for technical assistance, J.M. Farber for gift of a reagent, R.J. Kryscio for statistical guidance, and B. Appukuttan, M.W. Fannon, R. Mohan, A.P. Pearson, A.M. Rao, G.S. Rao, and K. Ambati for discussions. J.A. was supported by NEI/NIH, Doris Duke Distinguished Clinical Scientist Award, Burroughs Wellcome Fund Clinical Scientist Award in Translational Research, Macula Vision Research Foundation, E. Matilda Ziegler Foundation for the Blind, Dr. E. Vernon Smith and Eloise C. Smith Macular Degeneration Endowed Chair, Lew R. Wassermann Merit & Physician Scientist Awards (Research to Prevent Blindness-RPB), American Health Assistance Foundation, and departmental unrestricted grant from RPB; J.Z.B. by University of Kentucky Physician Scientist Award; M.E.K by International Retinal Research Foundation Dr. Charles Kelman Postdoctoral Scholar Award; R.J.C.A by Fight for Sight; B.K.A. by NEI/NIH, VA Merit Award, and Department of Defense; M.E.R. by NHLBI/NIAID/NIDDK/NIH and RPB departmental unrestricted grant; C.G. by NIAID/NHLBI; M.E.H. by NEI/NIH; and J.R.S. by NEI/NIH, and RPB Career Development Award and departmental unrestricted grant.

References

1. Ambati J, Ambati BK, Yoo SH, Ianchulev S, Adamis AP. Age–related macular degeneration: etiology, pathogenesis, and therapeutic strategies. Surv Ophthalmol. 2003; 48:257–293. [PubMed: 12745003]
2. Gragoudas ES, Adamis AP, Cunningham ET Jr, Feinsod M, Guyer DR. Pegaptanib for neovascular age-related macular degeneration. N Engl J Med. 2004; 351:2805–2816. [PubMed: 15625332]
3. Brown DM, et al. Ranibizumab versus verteporfin for neovascular age-related macular degeneration. N Engl J Med. 2006; 355:1432–1444. [PubMed: 17021319]
4. Rosenfeld PJ, et al. Ranibizumab for neovascular age-related macular degeneration. N Engl J Med. 2006; 355:1419–1431. [PubMed: 17021318]
5. Famiglietti EV, et al. Immunocytochemical localization of vascular endothelial growth factor in neurons and glial cells of human retina. Brain Res. 2003; 969:195–204. [PubMed: 12676380]

6. Nishijima K, et al. Vascular endothelial growth factor-A is a survival factor for retinal neurons and a critical neuroprotectant during the adaptive response to ischemic injury. Am J Pathol. 2007; 171:53–67. [PubMed: 17591953]
7. Saint-Geniez M, et al. Endogenous VEGF is required for visual function: evidence for a survival role on muller cells and photoreceptors. PLoS ONE. 2008; 3:e3554. [PubMed: 18978936]
8. Rothenberg ME, Hogan SP. The eosinophil. Annu Rev Immunol. 2006; 24:147–174. [PubMed: 16551246]
9. Grossniklaus HE, et al. Histopathologic and ultrastructural features of surgically excised subfoveal choroidal neovascular lesions: submacular surgery trials report no. 7. Arch Ophthalmol. 2005; 123:914–921. [PubMed: 16009831]
10. Justice JP, et al. Ablation of eosinophils leads to a reduction of allergen-induced pulmonary pathology. Am J Physiol Lung Cell Mol Physiol. 2003; 284:L169–178. [PubMed: 12388345]
11. Humbles AA, et al. A critical role for eosinophils in allergic airways remodeling. Science. 2004; 305:1776–1779. [PubMed: 15375268]
12. Pope SM, Zimmermann N, Stringer KF, Karow ML, Rothenberg ME. The eotaxin chemokines and CCR3 are fundamental regulators of allergen-induced pulmonary eosinophilia. J Immunol. 2005; 175:5341–5350. [PubMed: 16210640]
13. Jose PJ, et al. Eotaxin: a potent eosinophil chemoattractant cytokine detected in a guinea pig model of allergic airways inflammation. J Exp Med. 1994; 179:881–887. [PubMed: 7509365]
14. Teixeira MM, et al. Chemokine-induced eosinophil recruitment. Evidence of a role for endogenous eotaxin in an in vivo allergy model in mouse skin. J Clin Invest. 1997; 100:1657–1666. [PubMed: 9312163]
15. Blanchard C, et al. Eotaxin-3 and a uniquely conserved gene-expression profile in eosinophilic esophagitis. J Clin Invest. 2006; 116:536–547. [PubMed: 16453027]
16. Salcedo R, et al. Eotaxin (CCL11) induces in vivo angiogenic responses by human CCR3+ endothelial cells. J Immunol. 2001; 166:7571–7578. [PubMed: 11390513]
17. Puxeddu I, et al. Human peripheral blood eosinophils induce angiogenesis. Int J Biochem Cell Biol. 2005; 37:628–636. [PubMed: 15618019]
18. Heissig B, et al. Low-dose irradiation promotes tissue revascularization through VEGF release from mast cells and MMP-9-mediated progenitor cell mobilization. J Exp Med. 2005; 202:739–750. [PubMed: 16157686]
19. Tobe T, et al. Targeted disruption of the FGF2 gene does not prevent choroidal neovascularization in a murine model. Am J Pathol. 1998; 153:1641–1646. [PubMed: 9811357]
20. Nozaki M, et al. Drusen complement components C3a and C5a promote choroidal neovascularization. Proc Natl Acad Sci U S A. 2006; 103:2328–2333. [PubMed: 16452172]
21. Nozaki M, et al. Loss of SPARC-mediated VEGFR-1 suppression after injury reveals a novel antiangiogenic activity of VEGF-A. J Clin Invest. 2006; 116:422–429. [PubMed: 16453023]
22. Kleinman ME, et al. Sequence- and target-independent angiogenesis suppression by siRNA via TLR3. Nature. 2008; 452:591–597. [PubMed: 18368052]
23. Sakurai E, Anand A, Ambati BK, van Rooijen N, Ambati J. Macrophage depletion inhibits experimental choroidal neovascularization. Invest Ophthalmol Vis Sci. 2003; 44:3578–3585. [PubMed: 12882810]
24. Sakurai E, et al. Targeted disruption of the CD18 or ICAM-1 gene inhibits choroidal neovascularization. Invest Ophthalmol Vis Sci. 2003; 44:2743–2749. [PubMed: 12766082]
25. Humbles AA, et al. The murine CCR3 receptor regulates both the role of eosinophils and mast cells in allergen-induced airway inflammation and hyperresponsiveness. Proc Natl Acad Sci U S A. 2002; 99:1479–1484. [PubMed: 11830666]
26. Rothenberg ME, MacLean JA, Pearlman E, Luster AD, Leder P. Targeted disruption of the chemokine eotaxin partially reduces antigen-induced tissue eosinophilia. J Exp Med. 1997; 185:785–790. [PubMed: 9034156]
27. Kitamura Y, Go S, Hatanaka K. Decrease of mast cells in W/Wv mice and their increase by bone marrow transplantation. Blood. 1978; 52:447–452. [PubMed: 352443]

28. Zhou J, et al. Neutrophils promote experimental choroidal neovascularization. Mol Vis. 2005; 11:414–424. [PubMed: 15988410]
29. Fulkerson PC, et al. Negative regulation of eosinophil recruitment to the lung by the chemokine monokine induced by IFN-gamma (Mig, CXCL9). Proc Natl Acad Sci U S A. 2004; 101:1987–1992. [PubMed: 14769916]
30. Fulkerson PC, Zhu H, Williams DA, Zimmermann N, Rothenberg ME. CXCL9 inhibits eosinophil responses by a CCR3- and Rac2-dependent mechanism. Blood. 2005; 106:436–443. [PubMed: 15802529]
31. Green WR, Key SN 3rd. Senile macular degeneration: a histopathologic study. Trans Am Ophthalmol Soc. 1977; 75:180–254. [PubMed: 613523]
32. Ambati J, et al. An animal model of age-related macular degeneration in senescent Ccl-2- or Ccr-2-deficient mice. Nat Med. 2003; 9:1390–1397. [PubMed: 14566334]
33. Ip MS, et al. Anti-vascular endothelial growth factor pharmacotherapy for age-related macular degeneration: a report by the American Academy of Ophthalmology. Ophthalmology. 2008; 115:1837–1846. [PubMed: 18929163]
34. Sayanagi K, Sharma S, Kaiser PK. Photoreceptor Status after Anti-vascular Endothelial Growth Factor Therapy In Exudative Age-related Macular Degeneration. Br J Ophthalmol. 2009; 93:622–6. [PubMed: 19208677]
35. Yodoi Y, et al. Central Retinal Sensitivity After Intravitreal Injection of Bevacizumab for Myopic Choroidal Neovascularization. Am J Ophthalmol. 2009; 147:816–824. [PubMed: 19211092]
36. Carmeliet P, et al. Abnormal blood vessel development and lethality in embryos lacking a single VEGF allele. Nature. 1996; 380:435–439. [PubMed: 8602241]
37. Ferrara N, et al. Heterozygous embryonic lethality induced by targeted inactivation of the VEGF gene. Nature. 1996; 380:439–442. [PubMed: 8602242]
38. Marneros AG, et al. Vascular endothelial growth factor expression in the retinal pigment epithelium is essential for choriocapillaris development and visual function. Am J Pathol. 2005; 167:1451–1459. [PubMed: 16251428]
39. Bressler SB, Maguire MG, Bressler NM, Fine SL. Relationship of drusen and abnormalities of the retinal pigment epithelium to the prognosis of neovascular macular degeneration. The Macular Photocoagulation Study Group. Arch Ophthalmol. 1990; 108:1442–1447. [PubMed: 1699513]
40. Macular Photocoagulation Study Group. Risk factors for choroidal neovascularization in the second eye of patients with juxtafoveal or subfoveal choroidal neovascularization secondary to age-related macular degeneration. Arch Ophthalmol. 1997; 115:741–747. [PubMed: 9194725]
41. St Croix B, et al. Genes expressed in human tumor endothelium. Science. 2000; 289:1197–1202. [PubMed: 10947988]
42. Zhang L, et al. Gene expression profiles in normal and cancer cells. Science. 1997; 276:1268–1272. [PubMed: 9157888]
43. Wenzel SE. Eosinophils in asthma-closing the loop or opening the door? N Engl J Med. 2009; 360:1026–1028. [PubMed: 19264692]
44. Geisen P, McColm JR, Hartnett ME. Choroidal endothelial cells transmigrate across the retinal pigment epithelium but do not proliferate in response to soluble vascular endothelial growth factor. Exp Eye Res. 2006; 82:608–619. [PubMed: 16259980]
45. Peterson LJ, Wittchen ES, Geisen P, Burridge K, Hartnett ME. Heterotypic RPE-choroidal endothelial cell contact increases choroidal endothelial cell transmigration via PI 3-kinase and Rac1. Exp Eye Res. 2007; 84:737–744. [PubMed: 17292356]
46. Smith JR, et al. Unique gene expression profiles of donor-matched human retinal and choroidal vascular endothelial cells. Invest Ophthalmol Vis Sci. 2007; 48:2676–2684. [PubMed: 17525199]
47. Zamora DO, et al. Proteomic profiling of human retinal and choroidal endothelial cells reveals molecular heterogeneity related to tissue of origin. Mol Vis. 2007; 13:2058–2065. [PubMed: 18079679]

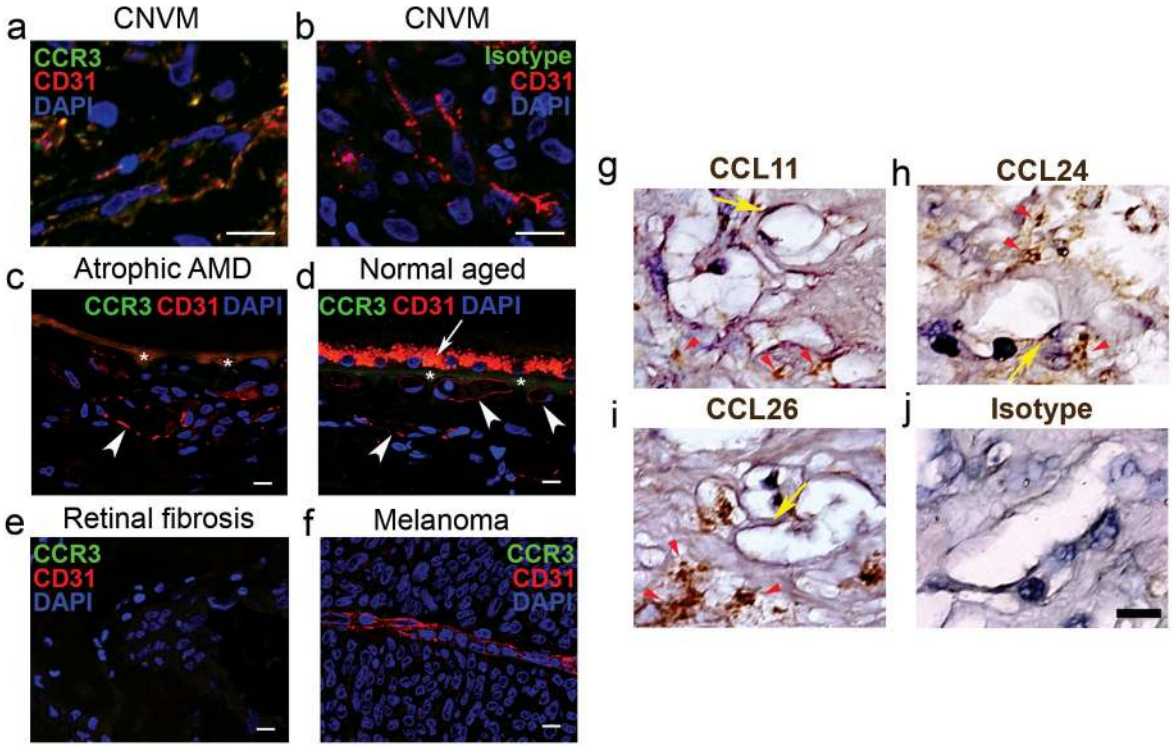

Fig. 1.

CCR3 and eotaxins are expressed in choroidal neovascularization. **a,b,** Immunofluorescence shows that CCR3 (green) receptor expression colocalizes with $CD31^+$ (red) expressing blood vessels in surgically excised human age-related macular degeneration (AMD) choroidal neovascular (CNV) tissue. Nuclei stained blue by DAPI. **b,** Specificity of CCR3 staining is confirmed by absence of staining with isotype control IgG (**a**). Individual red and green fluorescence channels are shown in Supplementary Fig. S1. **c,d,** CCR3 is not immunolocalized in $CD31^+$ (red) blood vessels (white arrowheads) in the choroid of patients with atrophic AMD who do not have CNV (**c**) or in aged patients without AMD (**d**). Autofluorescence of retinal pigmented epithelium (white arrow) and Bruch's membrane (asterisks) overlying choroid is seen (**c,d**). **e,f,** CCR3 is not expressed in surgically excised avascular retinal fibrosis tissue (**e**) or in blood vessel of choroidal melanoma (**f**). **g-j,** Immunohistochemistry (golden brown reaction product) shows expression of CCL11 (**g**), CCL24 (**h**), and CCL26 (**i**) in surgically excised AMD CNV tissue, primarily in the stroma (red arrowheads) but also in the blood vessels (yellow arrows). Specificity of staining is confirmed by absence of staining with isotype control IgG (**j**). Scale bars, 10 μm.

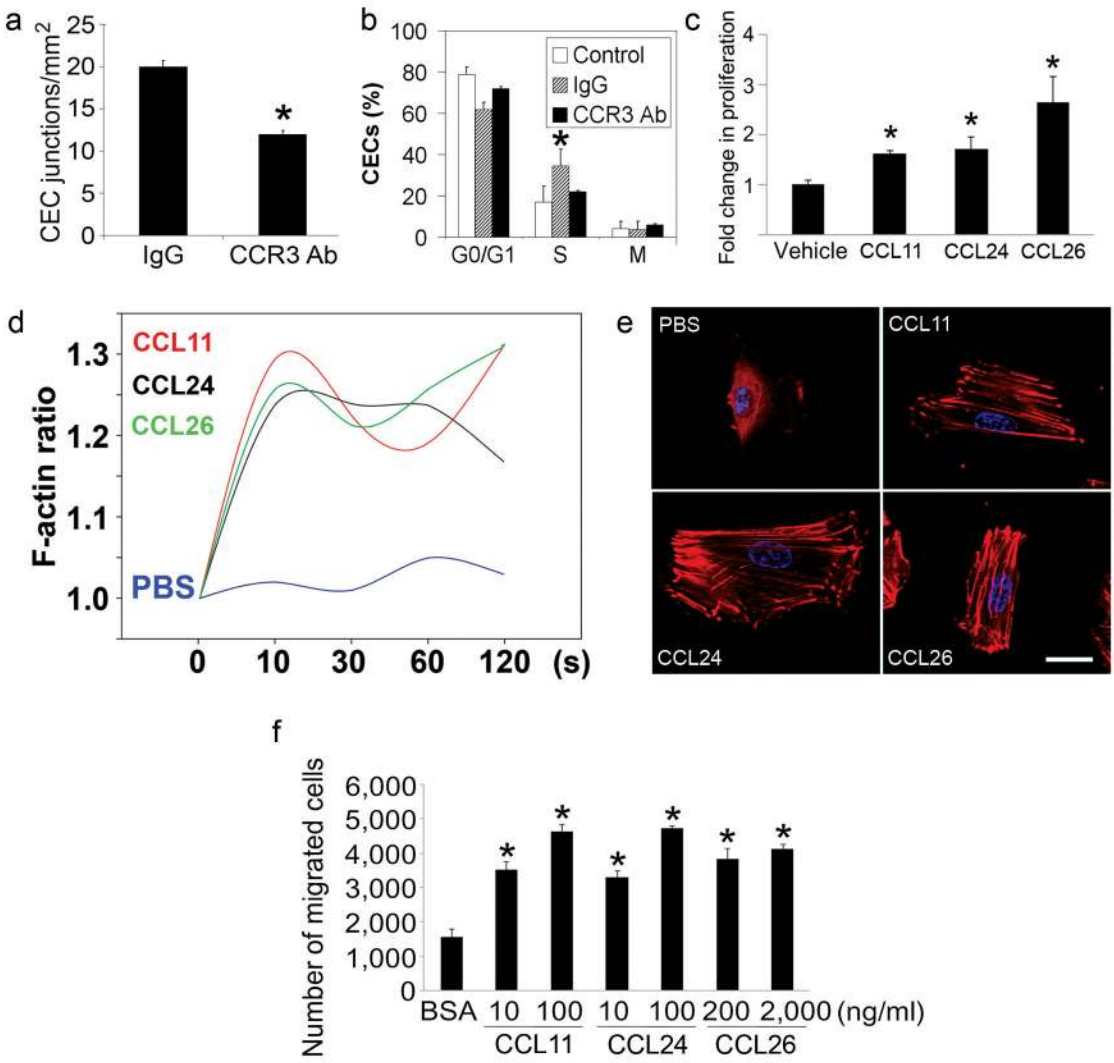

Fig. 2.

CCR3 activation promotes angiogenesis. **a,** Tube formation of primary human choroidal endothelial cells (CECs) in Matrigel *in vitro* was reduced by neutralizing anti-human CCR3 antibodies (Ab) compared to isotype IgG. n = 6, * $P < 0.05$ compared to isotype IgG. **b,** Fraction of $CD31^{+}VEGFR2^{+}$ gated mouse CECs *in vivo* in proliferative state (S phase) was increased 5 days after laser injury in wild-type mouse eyes compared to control (uninjured eyes), and was reduced by intraocular administration of neutralizing anti-mouse CCR3 Ab compared to isotype IgG. n = 6–10, * $P < 0.05$ compared to IgG treatment. **c,** Stimulation with eotaxins for 24 h induced human CEC proliferation. n = 4, * $P < 0.05$ compared to bovine serum albumin (BSA) treatment. **d,e,** Stimulation with eotaxins, but not PBS, induced actin polymerization in human CECs. Relative F-actin content is expressed as the ratio of the mean channel fluorescence between eotaxin- and media alone-stimulated cells (**d**). Rhodamine-phalloidin staining (red) shows F-actin fibre formation in eotaxin-stimulated cells (**e**). Nuclei stained blue by DAPI. Data representative of 3–4 independent experiments are shown. **c,e,** CCL11 (10 ng/ml), CCL24 (100 ng/ml), CCL26 (2 μg/ml). **f,**

Stimulation with eotaxins for 16 hours induces dose-dependent migration of human CECs across 8 μm pore size Transwells. n = 5–10, * $P < 0.05$ compared to BSA treatment. (**a–c, f**) Significance by Mann-Whitney U test. Error bars depict s.e.m.

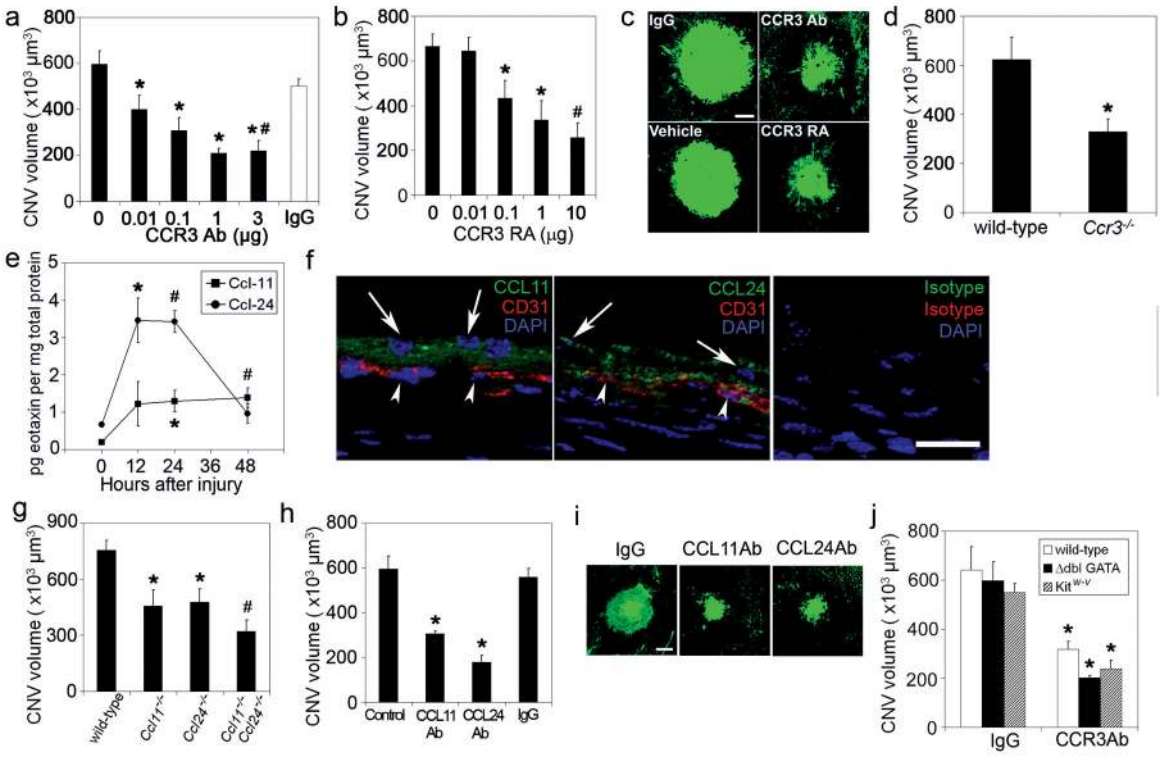

Fig. 3.

CNV reduced by CCR3 or eotaxin ablation or blockade independent of leukocyte modulation. **a,b,** Laser-induced CNV in wild-type mice was reduced by neutralizing anti-mouse CCR3 Ab compared to isotype IgG (**a**) and by the CCR3 receptor antagonist (RA) SB328437 ((S)-Methyl-2-naphthoylamino-3-(4-nitrophenyl)propionate) compared to vehicle (PBS/DMSO) (**b**) in a dose-dependent fashion. n = 8–12, * $P < 0.05$ compared to no antibody or receptor antagonist. **c,** Representative examples of CNV in drug-treated mice. **d,** Laser-induced CNV was reduced in *Ccr3*$^{-/-}$ mice compared to wild-type mice. n = 9, * $P <$ 0.05 compared to wild-type mice. **e,** Eotaxin-1 (Ccl-11) and eotaxin-2 (Ccl-24) protein levels, measured by ELISA, were increased following laser injury in wild-type mice. n = 6, * $P < 0.05$, # $P < 0.01$ compared to 0 h baseline. **f,** Ccl-11 and Ccl-24 immunofluorescence (green) was localized in the retinal pigmented epithelial cell layer (arrows) adjacent to CD31+ (red) choroidal endothelial cells (arrowheads) on day 1 after laser injury in wild-type mice. Nuclei stained blue by DAPI. No specific immunofluorescence was detected with isotype control IgGs. Images representative of 3 independent experiments are shown. **g,** Laser-induced CNV was reduced in *Ccl11*$^{-/-}$ and in *Ccl24*$^{-/-}$ mice compared to wild-type mice. n = 8–10, * $P < 0.05$ compared to wild-type mice. CNV is further reduced in *Ccl11*$^{-/-}$ × *Ccl24*$^{-/-}$ mice compared to single null mice. # $P < 0.05$ compared to single null mice. **h,** Laser-induced CNV in wild-type mice was reduced by neutralizing antibodies against mouse CCL11 or CCL24 compared to isotype IgG. n = 7–10, * $P < 0.05$ compared to no injection (control) or IgG. **i,** Representative examples of CNV in eotaxin-neutralized mice. **j,** Neutralizing anti-CCR3 antibodies (Ab) reduced laser-induced CNV in mice deficient in

eosinophils (Δdbl GATA) or mast cells ($Kit^{W\text{-}V}$). n = 6–9, * $P < 0.05$ compared to IgG. Scale bars, (**c,i**), 100 μm; **f**, 20 μm. Error bars depict s.e.m.

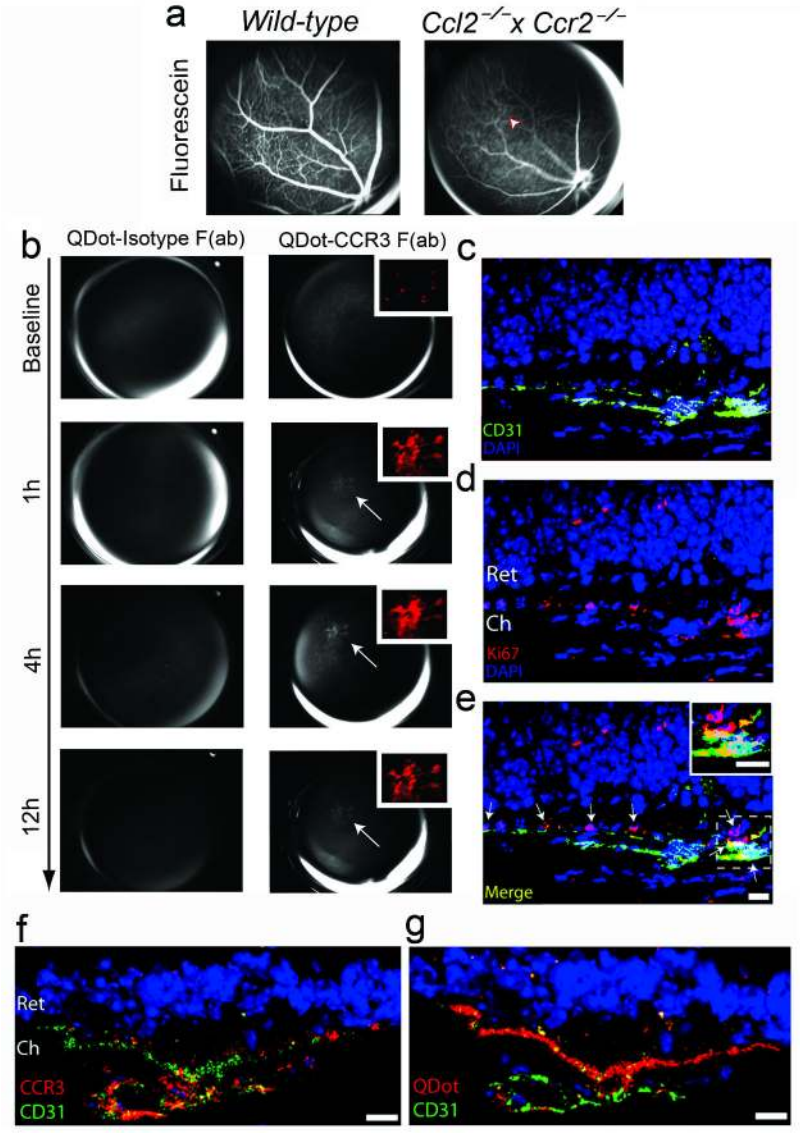

Fig. 4.

CCR3-targeting quantum dots detect subretinal choroidal neovascularization (CNV). **a,** Images of the fundus taken after intravenous injection of sodium fluorescein in wild-type and *Ccl2*$^{-/-}$ × *Ccr2*$^{-/-}$ mice showed normal retinal vascular filling but no areas of hyperfluorescence indicative of CNV. **b,** After intravenous injection of QDot-CCR3 Fab in the same *Ccl2*$^{-/-}$ × *Ccr2*$^{-/-}$ mouse shown in (**a**), focal branching choroidal hyperfluorescence was visualized (arrow) at 1 h in the same area that was not hyperfluorescent during fluorescein angiography (arrowhead in **a**). The intensity of this hyperfluorescence (shown in red pseudocolour in the inset) increased, attaining a peak at 4 h, and then declined in intensity but still persisted at 12 h. Corresponding images of QDot-Isotype Fab angiography showed no hyperfluorescence. **c–e,** The region corresponding to the area of hyperfluorescence seen on QDot-CCR3 Fab angiography in (**b**) contained multiple CD31^{+} blood vessels in the choroid (Ch) that were proliferating (Ki67^{+}; arrows)

and had not invaded the retina (Ret). Individual red ($CD31^+$, **c**), and green ($Ki67^+$, **d**), and merged (**e**) fluorescence channel images are shown. Arrows point to proliferating endothelial cells. Inset shows $Ki67^+$ $CD31^+$ cells in higher magnification. **f,** QDot-CCR3 Fab hyperfluorescent areas were localized to areas of subretinal CNV with $CCR3^+$ endothelial cells. **g,** The QDot label was visualized within $CD31^+$ vasculature of subretinal CNV lesions. Images representative of 6 independent experiments. Scale bars, (**c–e**), 10 μm.